Jefferson Lab
E01-012 Analysis Report 06
April 2005

Target polarization from EPR polarimetry during E01-012

P. Solvignon
Temple University, Philadelphia, PA 19122

E-mail
solvigno@jlab.org

Abstract

The different steps of the target polarimetry analysis for E01-012 are presented in this note.

1 Introduction

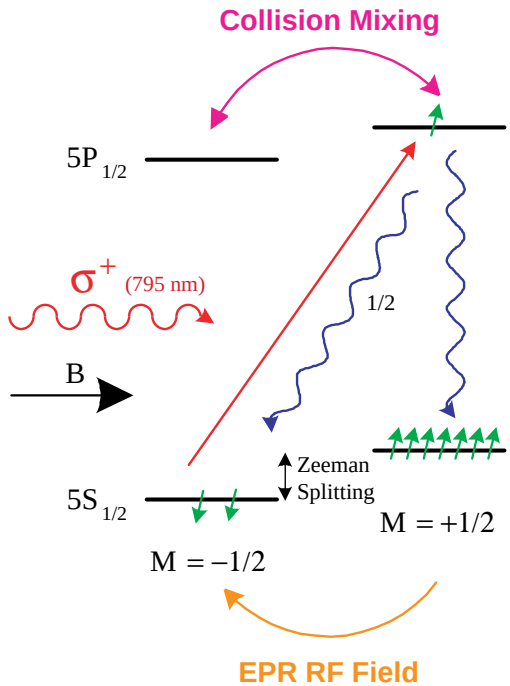

Figure 1: Optical pumping principle

Polarized ^{3}He nuclei created on small magnetic field $\delta B_{^3\mathrm{He}}$ increasing the Zeeman splitting between the sublevels of the Rb atoms. The transition frequency between these sublevels is proportional to the external field and in our case: $B_0 + \delta B_{^3\mathrm{He}}$, where B_0 is the holding field. Using an RF coil, the resonance frequency can be found for the external field $B_0 + \delta B_{^3\mathrm{He}}$ and then, by flipping the ^{3}He spins, we can access the resonance frequency for the external field B_0 - $\delta B_{^3\mathrm{He}}$. Therefore the polarization of the target is proportional to the resonance frequency shift:

$$P_{^3\mathrm{He}} = \frac{1}{\kappa_{\mathrm{EPR}}} \frac{\Delta\nu}{2} \tag{1}$$

κ_{EPR} depends on the external field, the density and the temperature of the pumping chamber.

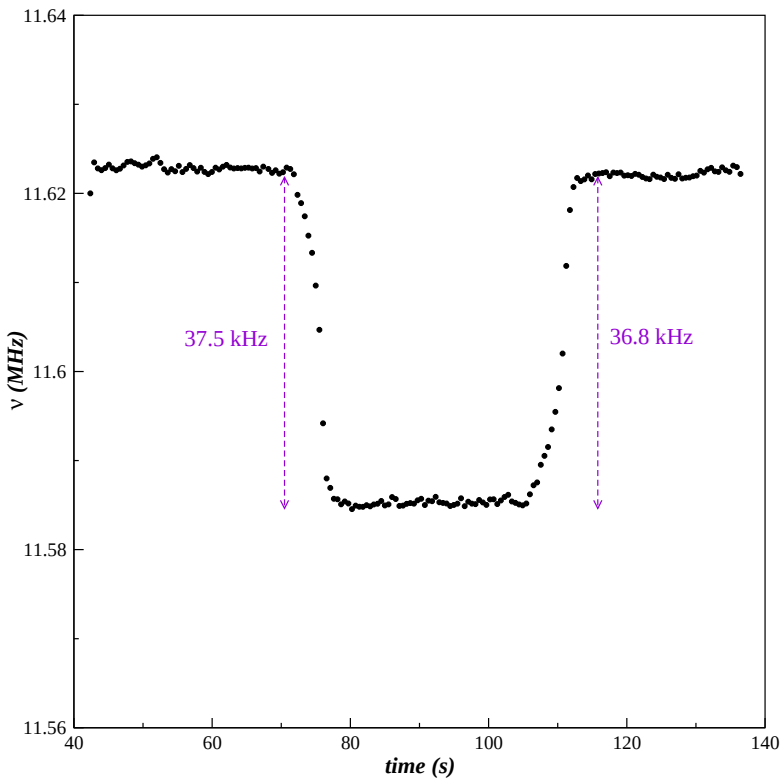

Figure 2: EPR measurement spectrum

2 Holding field

2.1 from Helmholtz coils calibration

A calibration of the Helmholtz coils was performed at the beginning of the experiment and the results are:

$$B_x = -3.45228 \cdot I_{large} - 0.1759 \tag{2}$$

$$B_z = 3.51139 \cdot I_{small} - 0.00346 \tag{3}$$

I_{small} and I_{large} are the current in the small (longitudinal) and the large (transverse) coils respectively. Due to the fact that the Helmholtz coils were not for purely longitudinal and transverse directions, both set of coils were

used to have the ^{3}He spins in longitundinal or tranverse. Thus the norm of the holding field is determined by:

$$B_0 = \sqrt{B_x^2 + B_z^2} \tag{4}$$

Figure 3 shows the holding field value calculated from eq. 2-4 when EPR

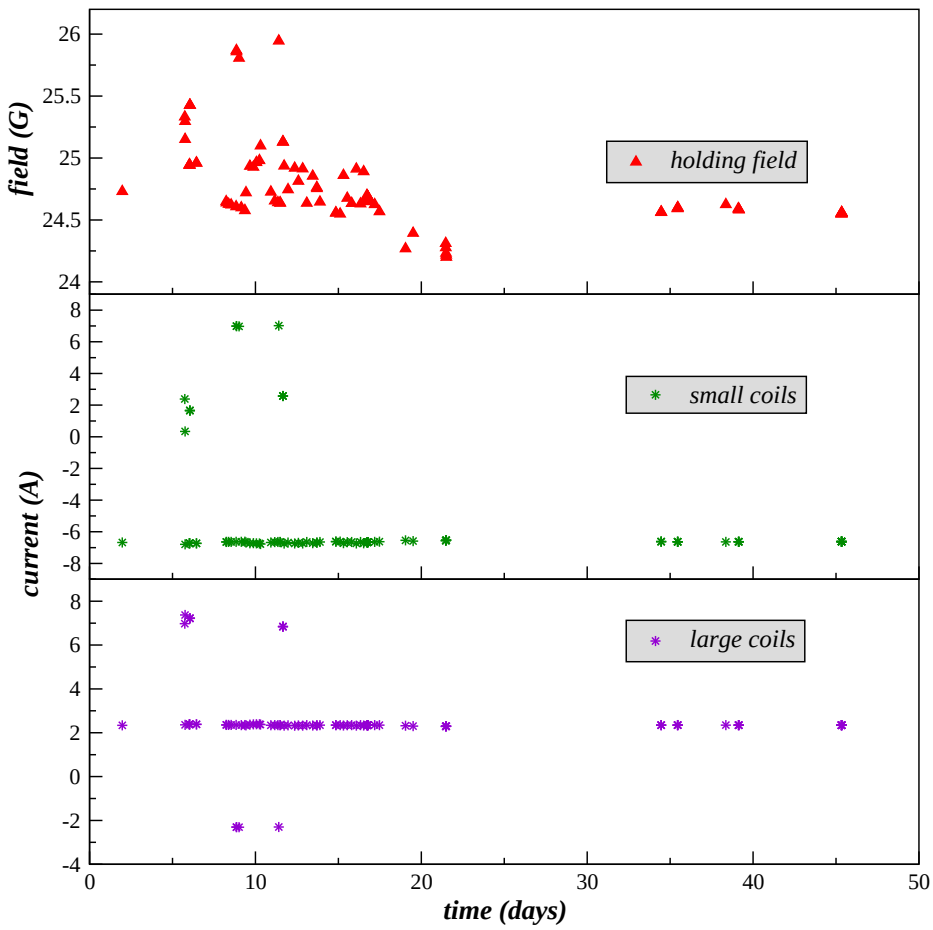

Figure 3: Holding field magnitude from Helmholtz coil currents.

measurements were performed. However, the power supply of one pair of Helmholtz coils failed during the preparation of the experiment and there was not enough time to recalibrate the coils with the new power supply.

In order to check the Helmholtz coil calibration validity, B_0 can be also determined using the EPR resonance frequency.

2.2 from EPR resonance frequency

In our polarized ^{3}He system, the holding field is about 25G. In this scenario, the Zeeman splitting is smaller than the hyperfine splitting. The energy of the sublevels can be determined for ^{85}Rb (I=5/2,S=1/2) from the Breit-Rabi formula [1]:

$$E_{F,m_F} = -\frac{h\nu_{hf}}{2(2I+1)} - g_I\mu_N B_0 m_F \pm \frac{h\nu_{hf}}{2}\sqrt{1+\frac{4m_F}{2I+1}x+x^2} \tag{5}$$

where F= I + S is the total spin. During E01-012, the polarized light and the holding field were setup in order to populate the level -3. An RF field is applied in order to induce the transition between sublevels. Thus the magnitude of the external field can be extracted when the RF frequency hits the resonance [4].

$$\begin{aligned} h\nu_{res.} &= E_{3,-2} - E_{3,-3} \\ &= -g_I\mu_N B_0 + \frac{h\nu_{hf}}{2}\left[\sqrt{1-\frac{4}{3}x+x^2} - \sqrt{1-2x+x^2}\right] \end{aligned} \tag{6}$$

with $x = \frac{g_J\mu_B + g_I\mu_N}{h\nu_{hf}}$ $B_0 \simeq \frac{g_J\mu_B}{h\nu_{hf}}$ B_0 since $\frac{g_I\mu_N}{g_J\mu_B} \simeq \frac{1}{1800}$.

B_0 can be found by solving eq. 7 and with $x = 9.2297\cdot$ B_0(Gauss). Fig. 4 shows the holding field magnitude extracting from eq. 7 at different order precisions for each EPR measurement.

$$\frac{\nu_{res.}}{\nu_{hf}} = \frac{1}{6}x + \frac{5}{36}x^2 + \frac{1}{6}x^3 - \frac{1}{16}x^4 + O(x^5) \tag{7}$$

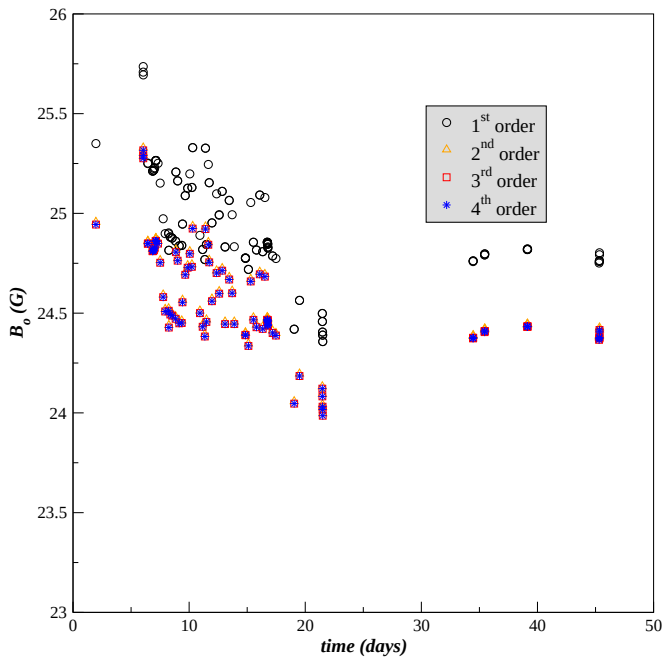

Figure 4: Holding field magnitude from EPR resonance. For the EPR analysis, we will use the 3rd order results.

2.3 Comparison of the two methods

The holding field magnitude from the two methods above is plotted on fig. 5. The discrepancy can be explained by all the other magnetic fields surrounding the target area (spectrometer magnets, earth field). Thus the second method is able to measure the external field felt by the spins with a very good precision.

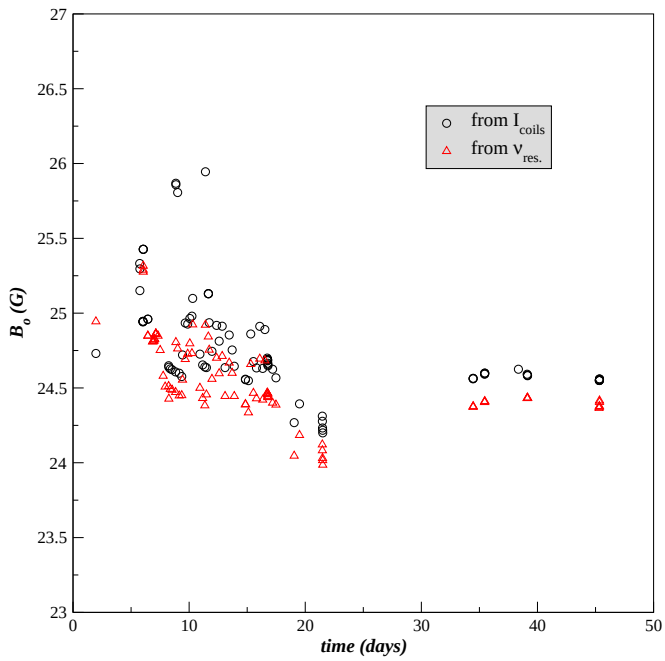

Figure 5: Comparison of the holding field magnitude extracting from Helmholtz coil calibration and from EPR resonance.

3 Determination of EPR constant

$$\kappa_{\mathrm{EPR}} = \frac{2}{3}\mu_0 \frac{\mathrm{d}\nu_{\mathrm{EPR}}(\mathrm{F}, \Delta \mathrm{m_f})}{\mathrm{dB}} \kappa_0 \mu_{^3\mathrm{He}} n_{^3\mathrm{He}} \tag{8}$$

with [4]:

$$\frac{\mathrm{d}\nu_{\mathrm{EPR}}(3, -2 \leftrightarrow -3)}{\mathrm{dB}} = 0.4670779 + 7.37904 \cdot 10^{-4}\mathrm{B} \tag{9}$$

and [2]:

$$\kappa_0 = 4.52 + 0.00934\ T \tag{10}$$

T is expressed in $^\circ C$. For each EPR measurement, RTD readout were extracted and the pumping chamber temperature and density could be calculated. We used the holding field magnitude from fig. 4. The EPR constant

κ_{EPR} for each EPR measurement is shown on fig. 6 as well as the holding field, the density $n_{^3\mathrm{He}}$ and the temperature T of the pumping chamber.

A recent measurement [3] of κ_0 is consistent with [2] for temperatures up to $350°C$:

$$\kappa_0 = 6.39 + 0.00914[T - 200] \tag{11}$$

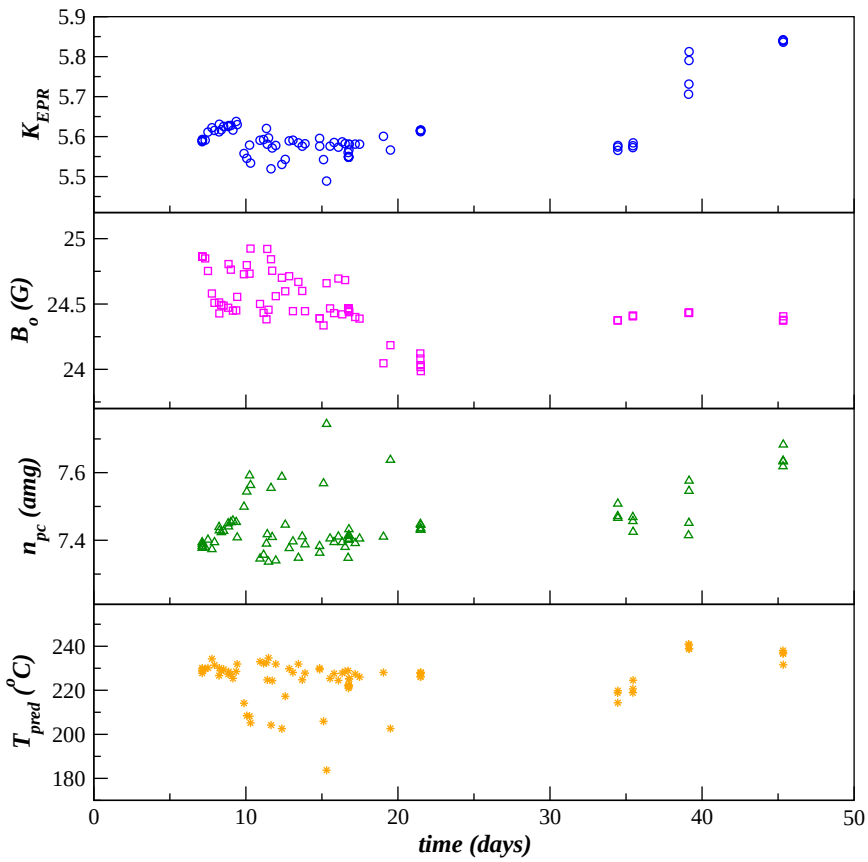

Figure 6: EPR constant.

4 Pumping chamber polarization

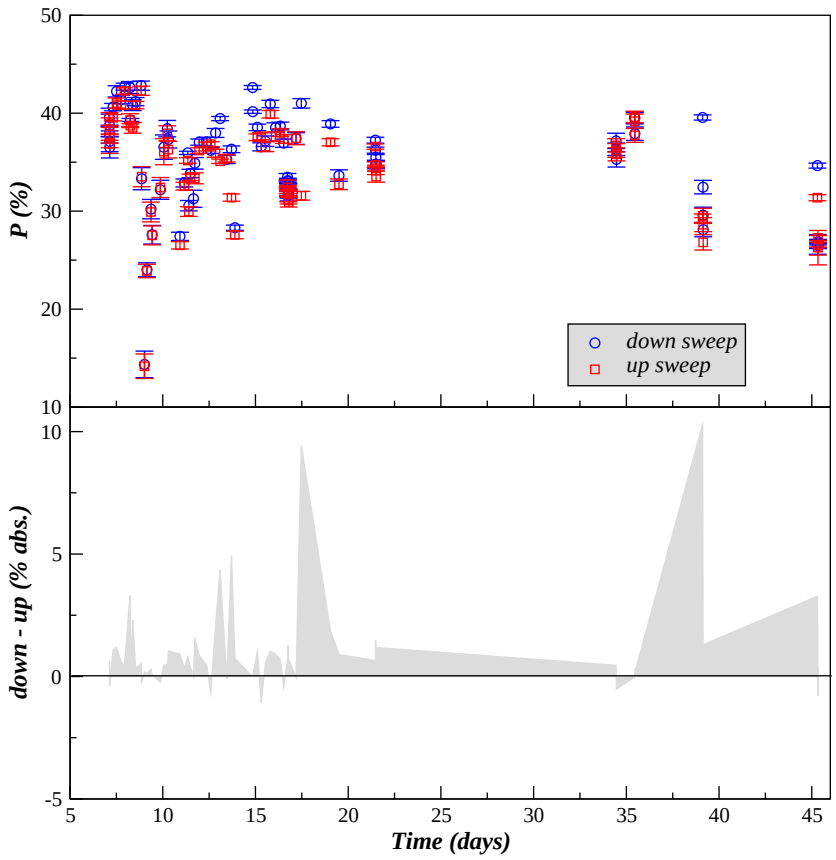

Figure 7: Comparison of polarization from up and down sweeps.

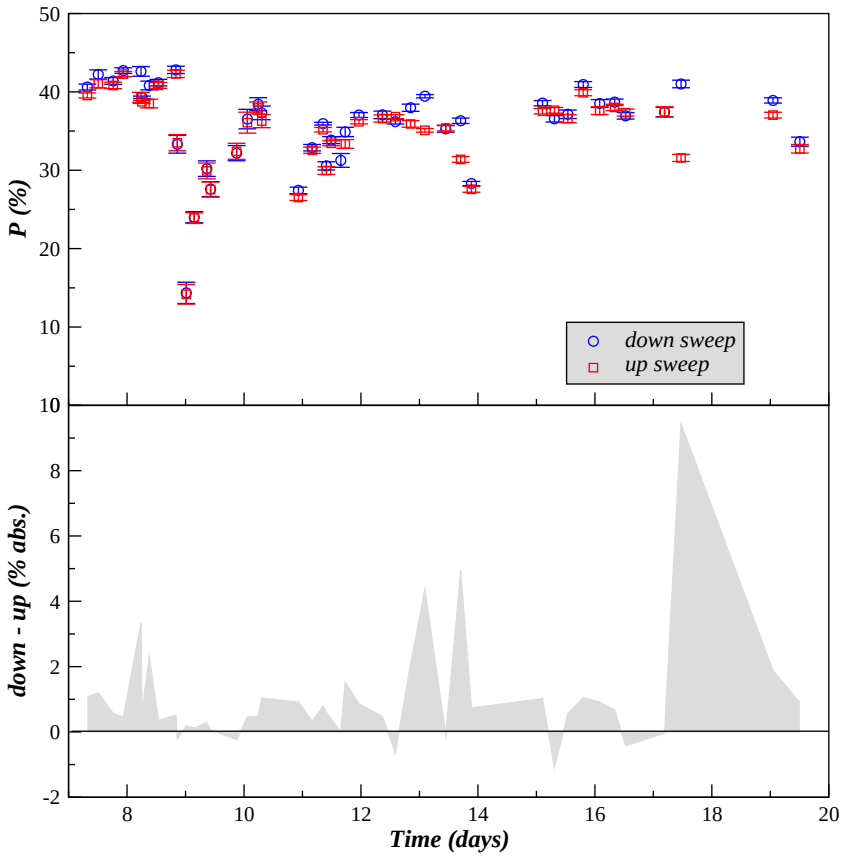

Figure 8: EPR constant.

5 Polarization gradient

Table 1: Cell characteristics

cell name	Duke	Exodus
τ_{cold} (h)	52.6	(44.1)
τ_{hot} (h)	26.2	none
P_{max} (%)	46.0	44.0
n_0 (amg)	9.18	9.62
V_{pc} (cm^3)	113.8	103.9
V_{tc} (cm^3)	82.6	84.7
dB_z/dz (mG/cm)	7.6	7.8

5.1 ^{3}He relaxation rates

- relaxation from holding field longitudinal gradient

$$\Gamma_{\Delta B} = 2D\frac{(dB_z/dz)}{B_0^2} \tag{12}$$

D $\simeq$ 0.2 cm^2/s: ^{3}He self-diffusion coefficient For a longitudinal gradient about 8mG/cm, $\Gamma_{\Delta B} \simeq 1.5 \times 10^{-4}$ h^{-1}. Thus it is negligeable.

- ^{3}He-^{3}He magnetic dipolar interaction

$$\Gamma_{dipolar} = \frac{[^3\mathrm{He}]}{744}\ \mathrm{h}^{-1} \tag{13}$$

- beam relaxation Since EPR measurements were not taken with the beam on, the beam relaxation is not included here.

- wall relaxation The total relaxation effect can be measured by fitting the spindown data and extracting the average lifetime of the cell:

$$\frac{1}{\tau} = \Gamma_{dipolar} + \Gamma_{wall} \tag{14}$$

During EPR measurement, the pumping chamber is at about 500K and the target chamber at about 320K. So a lifetime measurement done

when the target was at room temperature doesn't allow us to extimate the wall relaxation. In the EEL target test lab, a hot spindown was performed on Duke in July 2002. The target and pumping chamber densities was calculated from the temperature test done at the same period: $n_t = 11.8$amg and $n_p = 7.2$amg.

$$\Gamma_{wall}^{targ} = \frac{1}{\tau} - \Gamma_{dipolar}^{targ} = \frac{1}{45}\ \mathrm{h}^{-1} \tag{15}$$

$$\Gamma_{wall}^{pump} = \frac{1}{\tau} - \Gamma_{dipolar}^{pump} = \frac{1}{35}\ \mathrm{h}^{-1} \tag{16}$$

Duke and Exodus are made with the same glass (GE180) and their physical characteristics are not very different, we will consider that the wall relaxations are the same for both cells.

The spin relaxations rates will be determined for each EPR measurement from the densities of the target and pumping chamber as followed:

$$\Gamma_t = \frac{n_t}{744} + \frac{1}{45} \tag{17}$$

$$\Gamma_p = \frac{n_p}{744} + \frac{1}{35} \tag{18}$$

5.2 Rubidium concentration

T_{Rb} = temperature of the pumping chamber bottom = oven temperature = 170°C

6 EPR-NMR calibration constant

During Feb. 8 calibration, EPR showed large AFP loss. That might be due to masing. So this calibration can be ignored and the valid calibration for Exodus is the one from Feb. 14 where we made sure no masing will occur.

For Duke, the Jan. 7 calibration difference with the other calibration is due to the realignment of the lasers on Jan. 9. Otherwise, the three calibrations done after the realignment agree pretty well.

Table 2: EPR-NMR calibration constants (in %/mV).

cell name	date	$C_{EPR-NMR}$
Duke	Jan. 7	3.211 ± 0.060
	Jan. 16	3.300 ± 0.037
	Feb. 3	3.307 ± 0.046
	Feb. 4	3.314 ± 0.042
Exodus	Feb. 8	2.299 ± 0.043
	Feb. 14	2.426 ± 0.031

7 Target chamber polarization from EPR-NMR calibration

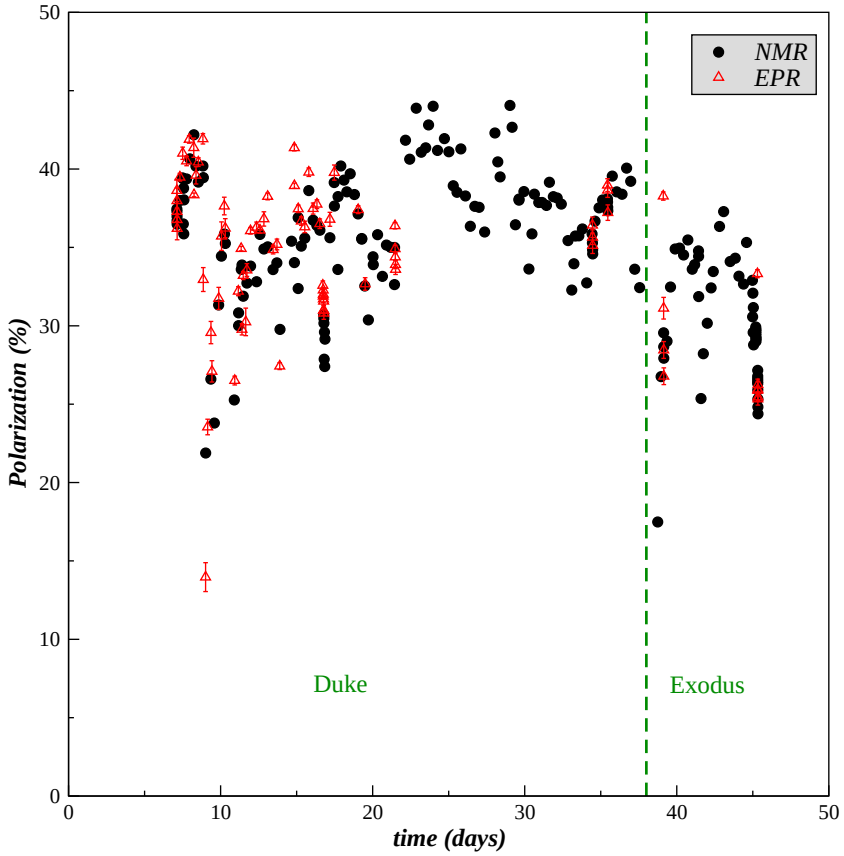

Figure 9: Target polarization using EPR-NMR calibration.

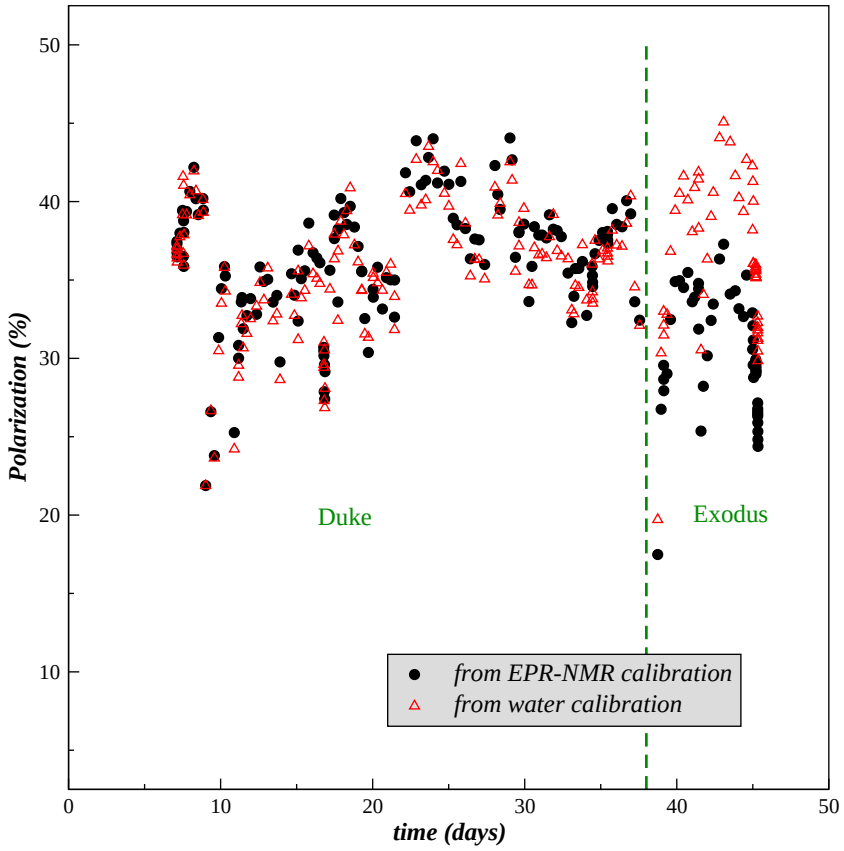

Figure 10: Comparison of the target polarization from EPR-NMR calibration and water calibration.

8 Masing

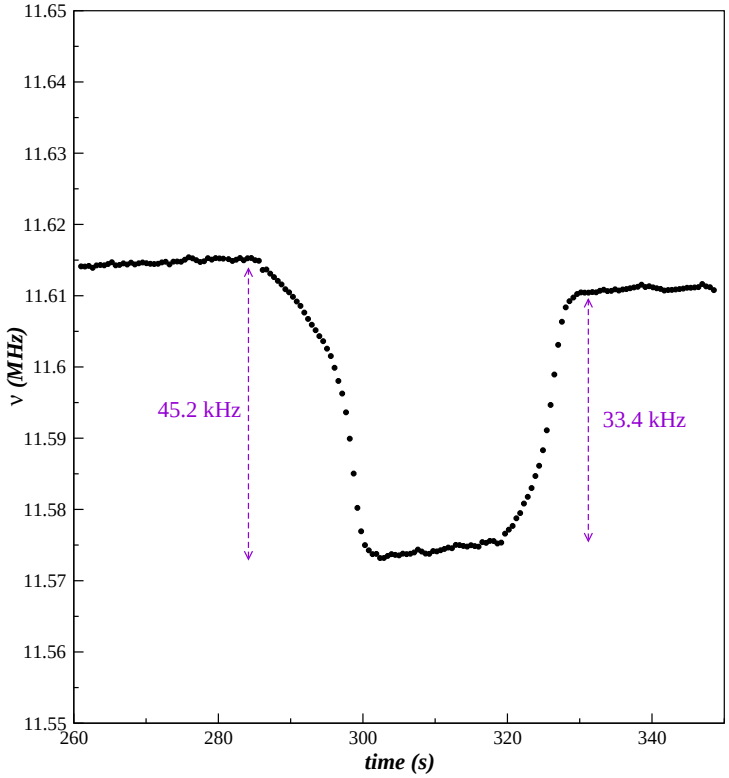

Figure 11: EPR measurement spectrum showing strong masing

References

[1] M.V. Romalis, Ph.D. thesis, Princeton University, 1997.

[2] M.V. Romalis *et al.*, Phys. Rev. **A39**, 5613 (1989).

[3] E. Babcock *et al.*, Phys. Rev. **A71**, 013414 (2005).

[4] W. Korsch, Technical note, E94010 Collaboration, (unpublished), 1998. http://www.jlab.org/e94010/, TN-E94010-11.